Journal of the Ceramic Society of Japan 118 [7] 575-578 2010 Paper

Selective growth of gold nanoparticles on FIB-induced amorphous phase of Si substrate

Tomoyo MATSUOKA, Masayuki NISHI,† Yasuhiko SHIMOTSUMA,*
Kiyotaka MIURA and Kazuyuki HIRAO

Department of Material Chemistry, Graduate School of Engineering, Kyoto University, Nishikyo-ku, Kyoto 615–8510
***Innovative Collaboration Center, Kyoto University, Nishikyo-ku, Kyoto 615–8510**

Maskless and electroless patterning of gold was performed by a simple method: 3-mercaptopropyltrimethoxysilane (MPTMS) and an aqueous solution of hydrogen tetrachloroaurate ($HAuCl_4 \cdot 4H_2O$) were reacted, and the obtained solution was dropped onto a silicon substrate processed by a focused ion beam (FIB). This method utilizes the selective growth of gold nanoparticles on an FIB-processed area of a silicon surface. Raman microspectroscopy revealed that gold nanoparticles selectively grew on an FIB-processed area when an amorphous silicon phase was induced by an FIB. Unlike other attempts to fabricate metal patterns with silane coupling agents, MPTMS acts as a reducing agent, not as glue.

Key-words : Metal patterning, Focused ion beam, Gold, Nano

[Received January 21, 2010; Accepted May 20, 2010]

1. Introduction

Metal patterning on a silicon surface has wide range of applications in electronics fields: Schottky diodes,[1] integrated circuits (IC),[2),3] through holes for printed boards,[4] and so on. This patterning is attracting increased attention because it can also be applied to wire grid polarizers for terahertz waves[5] and to surface plasmon resonance devices.[6]

Several types of metal-patterning methods have been reported in the past. The most common and well-known methods are photolithography for micropatterning and electron-beam lithography for nanopatterning. Both techniques are, however, indirect approaches and many steps are needed to obtain the target metal structures: coat Si substrate with resist film, modify parts of resist film using UV light (with masking) or an electron beam, remove either modified or unmodified parts selectively, deposit metal on substrate, and finally remove residual resist. In this final step, the metal structures deposited on the residual resist are removed together with the resist so that only the metal structures deposited directly on the Si surface are left. Methods for fabricating metal structures more easily by direct modifying of the Si surface (i.e., resistless and maskless processes) have thus been attracting much attention recently. Electrodeposition process is commonly involved in this approach.[7] This method utilizes high reactivity of the modified parts of Si surface for electrodeposition. Homma et al. reported a direct and electroless process[8] in which the surface of a hydrogen-terminated P-type Si wafer is directly modified by nanoindentation and then immersed into aqueous solution of $Cu(NO_3)_2$ and HF. Copper nanostructures selectively form at the nanoscopic defect sites, that is, the nanoindentation locations.

We previously reported a simple method for preparing single crystalline tabular gold microparticles with nanoscale thickness. An ethanol solution of 3-mercaptopropyltrimethoxysilane (MPTMS) is mixed with an aqueous solution of hydrogen tetrachloroaurate[9] ($HAuCl_4 \cdot 4H_2O$). Observation of the reaction products on an undoped Si wafer (single-sided; cut in pieces $\sim$1 cm^2) using a field-emission scanning electron microscope (FE-SEM) revealed one-dimensional (1D) arrays of gold nanoparticles ($\sim$10 nm in diameter) in addition to gold microplates. It was found that possibility of 1D arrays depends on the way to snap Si wafer off: the possibility is higher in snapping so that the polished surface is inside than in snapping so that the polished surface is outside. This phenomenon implied that the 1D arrays of gold nanoparticles were formed on the local active sites induced by stress generated by snapping. It was also found that gold nanoparticles selectively precipitate on the surface scratched intentionally and weakly by hand with a diamond pencil, but do not precipitate on that scratched strongly. This implies that there is an optimum stress for inducing active sites for arrays of gold nanoparticles.

Here, we have used a focused ion beam (FIB) to perform nano/micro processing and developed a direct and electroless method for gold patterning on a Si surface. In this work, the solution dropped on to the FIB-processed Si wafer was adjusted to grow only spherical nanoparticles on the FIB-processed area, which enabled us to inhibit the formation of tabular microparticles that were unfit for our purpose.

2. Experimental procedure

Our method for gold patterning consists of three steps, as shown in **Fig. 1**. Undoped Si (100) wafers, which were precleaned by sonication for 5 min in ethanol, were used. Geometric patterns were written on them with a Ga FIB (JEM-9310, JEOL, Japan) at 30 kV. A drop of prepared suspension was then dropped on the wafer, and the wafers were dried at 80°C. The suspension contained a mixture of 42.5 µl of MPTMS and 3 ml of 0.05 M aqueous solution of $HAuCl_4$ and was prepared by stirring on a hot plate set to 100°C for 2 hours.

A Raman microspectrometer (Nanofinder30, Tokyo Instruments, Japan; wavelength = 532 nm, NA = 0.6), a FE-SEM (JSM6700F, JEOL, Japan), and an energy dispersive X-ray

† Corresponding author: M. Nishi; E-mail: west@collon1.kuic.kyoto-u.ac.jp

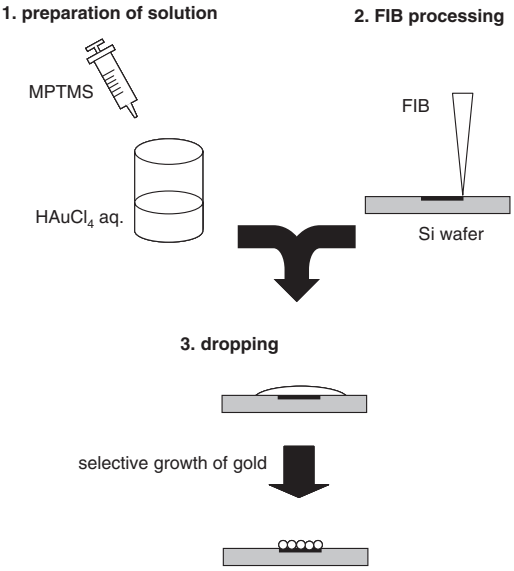

Fig. 1. Fabrication of gold patterns on Si substrate.

Table 1. Relationship between irradiation current and beam width for ten beams available

Beam	Irradiation current (pA)	Beam width (nm)
1	10000	600
2	5000	400
3	3000	300
4	1000	100
5	500	70
6	300	50
7	100	30
8	50	20
9	10	15
10	1	8

spectrometer (JED-2300, JEOL, Japan) were used to investigate the processed wafers and gold nanostructures.

Table 1 shows the relationship between the irradiation current and the beam width for the ten beams available with the FIB (JEM-9310). We chose beams: 2, 8, and 9 (this selection of beams has no special significance). To obtain an FIB-processed area large enough for Raman analysis, we processed the Si substrate using only the beam effect caused while scanning ion microscope (SIM) image is obtained (beam 2 for 30 seconds).

3. Results

Figure 2 shows a SEM image of a sample obtained using the beam with an irradiation current (IC) of 50 pA, a beam width (BW) of 20 nm, and an estimated dosage (ED) of 6.2×10^{16} ions/cm^2. **Figure 3** shows the result of energy dispersive X-ray spectrometer (EDS) line profile analysis for Au. As can be seen, the fabrication of gold patterns with high spatial selectivity was achieved.

Raman spectra for the FIB processed and unprocessed areas are shown in **Fig. 4**. The spectrum for the processed area (Fig. 4(b)) differed from that for the unprocessed area (Fig. 4(a)) and showed not only the peaks of crystalline silicon (known as Si-I) but also two other peaks (broad peaks at 470 and 150 cm^{-1}), which can be assigned as amorphous silicon. This phenomenon

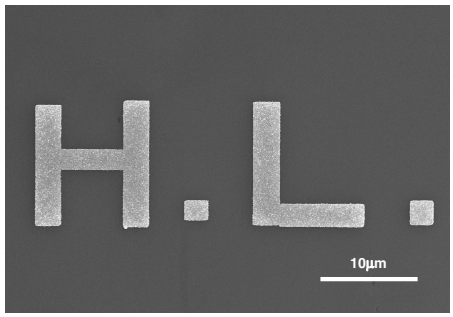

Fig. 2. FE-SEM image of obtained gold pattern.

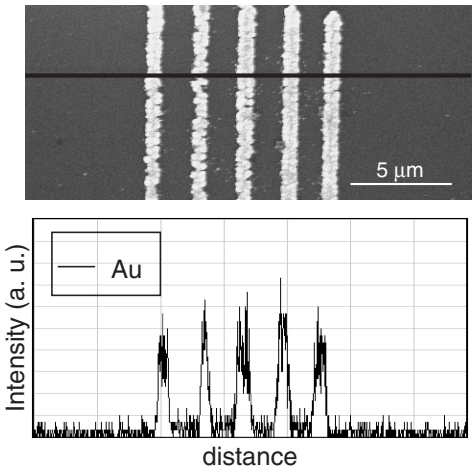

Fig. 3. EDS line profile analysis of obtained gold structure.

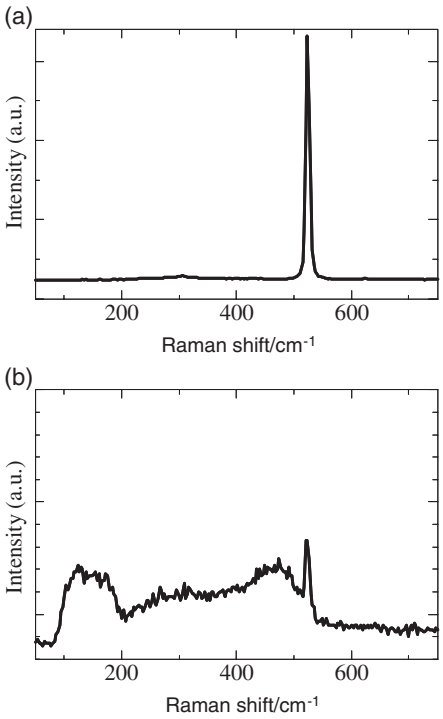

Fig. 4. Raman spectra of silicon used for gold patterning; (a) unprocessed area, (b) FIB processed area.

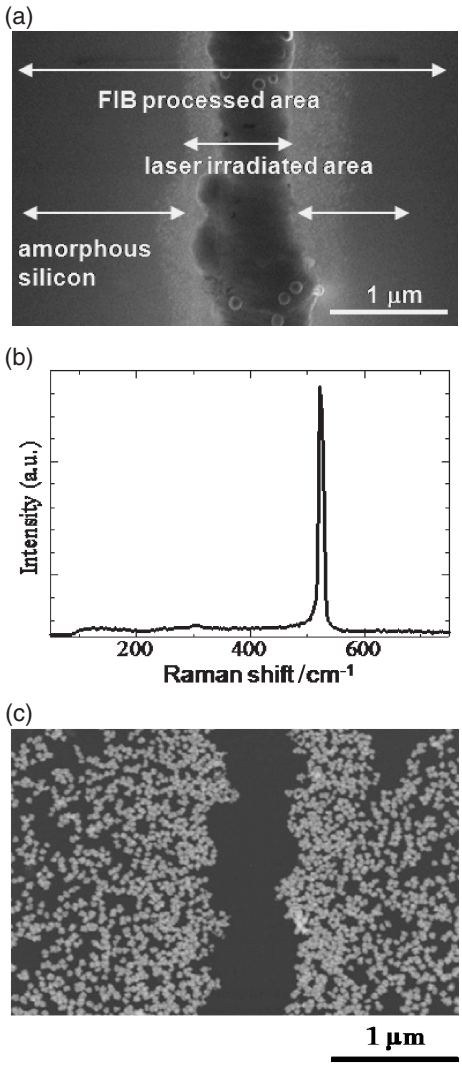

Fig. 5. (a) FE-SEM image of CW laser irradiated area in amorphous silicon induced by an FIB (b) Raman spectrum of CW laser irradiated area (c) FE-SEM backscattered electron image of the same area as in (a) but was observed after gold precipitation. This backscattered electron image reflects the compositional contrast.

(i.e., the transition of crystalline silicon to amorphous silicon due to FIB irradiation) was also reported by Rubanov and Munroe.[10)]

To investigate the importance of amorphous silicon in gold precipitation, a part of FIB-processed area was recrystallized and the procedure for gold precipitation was performed. Recrystallization of amorphous silicon was achieved by irradiation of tightly focused laser beam. The beam from an Nd:YAG CW laser with a wavelength of 532 nm can produce crystalline silicon phase from amorphous silicon.[11)] The numerical aperture (NA) of the objective lens used for this was 0.9, which is larger than that of the lens used for Raman analysis (NA = 0.6). **Figure 5**(a) shows a SEM image of a laser irradiated area on amorphous silicon induced by an FIB. The Raman spectrum of this area (Fig. 5(b)) indicates that the amorphous silicon was recrystallized by the laser irradiation. Figure 5(c) shows a backscattered electron image of the same area as Fig. 5(a) but was captured after gold precipitation. Gold nanoparticles were observed on the FIB-processed area (i.e., amorphous silicon area) but almost no gold nanoparticles in the laser-irradiated area (i.e., the recrystallized area).

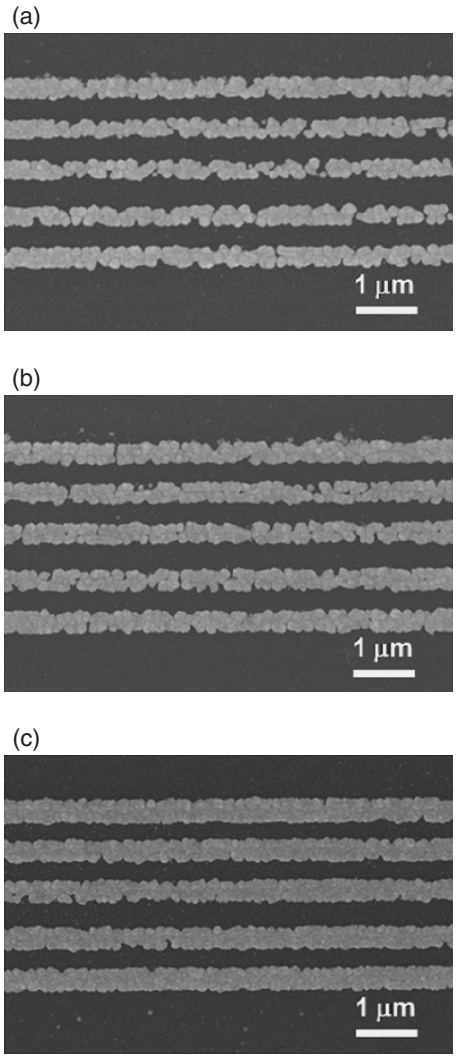

Fig. 6. FE-SEM images of gold structures obtained using beam9. Estimated dosages are (a) 1.2×10^{16}, (b) 1.2×10^{17}, and (c) 3.75×10^{17} ions/cm^2.

Figure 6 shows FE-SEM images of the gold structures for three FIB-processing times (i.e., dosages) created using beam 9 (IC = 10 pA, BW = 15 nm); (a) 1.2×10^{16}, (b) 1.2×10^{17}, and (c) 3.75×10^{17} ions/cm^2. These results indicate that, in this range of dosage, increasing the dosage increases the amount of gold structures.

4. Discussion

The results in Figs. 4 and 5 show that the amorphous phase plays an important role on the fabrication of gold nanostructures on silicon. The importance of the induced amorphous phase was also demonstrated by our results for scratching with a diamond pencil: We obtained 1D gold nanoparticle arrays on lines scratched by hand weakly with a diamond pencil but not on ones scratched strongly. In the same way as FIB, we have also confirmed using Raman microspectroscopy that the amorphous silicon phase was dominant in the area scratched weakly whereas little amorphous phase in the area scratched strongly (the data is not shown here). Similar phenomenon was reported by R. Gassilloud et al.[12)] Why is the amorphous phase important? Dangling bond defects may be an origin, because it is well-known that commercially available amorphous silicon is inten-

tionally terminated by hydrogen. We can expect that amorphous silicon induced by an FIB has a large number of active sites compared with crystalline silicon. Since the number of the active sites decreases considerably by laser annealing, it is difficult for gold to precipitate on the annealed area as shown in Fig. 5. The amorphization and damage level of ion-irradiated crystalline silicon have been investigated by other groups and they showed threshold-like increase in damage with increasing dosage.[13] This dependence of the damage on ion dosage is similar to the dependence of the number of precipitated gold nanoparticles on dosage in Fig. 6. Thus, significant contribution of the induced defects to the selective growth of gold nanoparticles is implied.

In our previous works, MPTMS worked as a reducing agent and produced gold particles in the solution containing aurate (III) ions.[9] In this work, we modulated the reaction conditions of MPTMS and aurate ion. This modulation resulted in a partial and incomplete reduction of aurate (III) ions: a large number of gold particles were identified after keeping the solution at 80°C for 24 h, whereas no change was observed when it was kept at room temperature. It is also noted that $HAuCl_4$ aqueous solution did not give us the gold pattern without MPTMS. We expect that partially reduced aurate ions can be completely reduced to gold nanoparticles once further energy or electrons are given from active sites of the FIB-processed area.

5. Conclusions

We applied our previous synthesizing method to fabricating patterned gold nanostructures on silicon wafer. Using FIB irradiation, we obtained gold patterns about 300 nm wide with high spatial selectivity. The fabricating process is very simple, and the overall process is maskless and electroless. This means that its use should reduce costs and open the door to new applications.

We also demonstrated that the presence of amorphous silicon is important for fabricating gold nanostructures. Future work will focus on understanding how the amorphous silicon and MPTMS work together.

Acknowledgment This research was supported in part by the Global COE Program “International Center for Integrated Research and Advanced Education in Materials Science” (No. B-09) of the Ministry of Education, Culture, Sports, Science and Technology (MEXT) of Japan, administrated by the Japan Society for the Promotion of Science.

References

1) M. Erhardt and R. Nuzzo, *Langmuir*, 15, 2188–2193 (1999).
2) P. C. Andricacos, C. Uzoh, J. O. Dukovic, J. Horkans and H. Deligianni, *IBM J. Res. Dev.*, 42, 567–574 (1998).
3) R. Rosenberg, D. C. Edelstein, C. K. Hu and K. P. Rodbell, *Annu. Rev. Mater. Sci.*, 30, 229–262 (2000).
4) E. K. Yung, L. T. Romankiw and R. C. Alkire, *J. Electrochem. Soc.*, 136, 206–215 (1989).
5) I. Yamada, K. Takano, M. Hangyo, M. Saito and W. Watanabe, *Opt. Lett.*, 34, 274–276 (2009).
6) M. L. Brongersma, J. W. Hartman and H. A. Atwater, *Phys. Rev. B*, 62, R16356–R16359 (2000).
7) P. Schmuki and L. E. Erickson, *Phys. Rev. Lett.*, 85, 2985–2988 (2000).
8) T. Homma, N. Kubo and T. Osaka, *Electrochim. Acta*, 48, 3115–3122 (2003).
9) M. Nishi, T. Nakanishi, Y. Shimotsuma, K. Miura and K. Hirao, *J. Ceram. Soc. Japan*, 115, 944–946 (2007).
10) S. Rubanov and P. R. Munroe, *J. Microsc.*, 214, 213–221 (2004).
11) J. C. C. Fan and H. J. Zeiger, *Appl. Phys. Lett.*, 27, 224–226 (1975).
12) R. Gassilloud, C. Ballif, P. Gasser, G. Buerki and J. Michler, *Phys. Status Solidi A*, 202, 2858–2869 (2005).
13) L. Pelaz, L. A. Marqués and J. Barbolla, *J. Appl. Phys.*, 96, 5947–5976 (2004).